Design of Reconfigurable Ultrawide Band Antenna with Switchable Single/Dual/Triple Band Notch Functions

Jian Dong, Shan Wang, and Guoqiang Hu

School of Information Science and Engineering
Central South University, Changsha, 410083, China
dongjian@csu.edu.cn

Abstract **─** A reconfigurable ultrawide band (UWB) antenna with switchable single, dual, and triple band notch functions is presented in this study. In the proposed structure, by etching slots on the radiating patch, the ground plane, and the feedline, triple band-notched characteristics at the WLAN, WiMAX and X-band frequencies are obtained. Then, by introducing switch modes on the slots, the antenna offers eight working modes and can realize an interconversion between one UWB mode, three single band-notched modes, three dual band-notched modes, and one triple band-notched mode. Simulated and measured results show that the proposed antenna can provide good band-notched functions on the stopbands and has nearly omnidirectional radiation patterns on the passbands.

Index Terms **─** Band-notched, reconfigurable antenna, slots, switch, ultrawide band (UWB) antenna.

I. INTRODUCTION

Ultrawide band (UWB) technology was used in military initially and has drawn more and more attention since the Federal Communications Commission (FCC)'s allocation of the frequency band 3.1-10.6 GHz for commercial use [1]. Compared to a narrow band system, UWB technology would be more attractive because of its wide transmission bandwidth, low transmission power, and high data transmission rates and so on. However, UWB systems have encountered a hostile radio environment which may cause potential interferences to the UWB band. For instance, IEEE 802.16 WiMAX system operates at 3.3–3.7 GHz; IEEE 802.11a WLAN system operates at 5.15–5.825 GHz and X-band satellite downlink signal operates at 7.25-7.75GHz, uplink signal operates at 7.9~8.4GHz. To solve this problem, it is desirable to design UWB antennas with intrinsic band-notched characteristic to suppress the interference from these narrow band systems [2].

Various methods for designing band-notched UWB antennas have been presented and reported. Designs of using parasitic stubs as resonators to achieve band-notched function were presented in [4-[7]. In these designs, the antenna structures cannot be compact enough due to the use of parasitic stubs. In order to make the structure of band-notched antenna more compact, etching slots such as L-shaped, C-shaped, E-shaped, H-shaped, and other slots on the radiating patch or on the ground plane was used to achieve band-notched function [8]-[18]. In [8], by etching a pair of inverted-L-shaped slots around the microstrip line on the ground, a frequency-notched function centered at 5.2 GHz is obtained. In [9], a rejected frequency band of 5-6 GHz is obtained by etching an H-shaped slot from the back patch of a conventional UWB antenna. In [10], the proposed antenna can obtain a UWB property with a 5.1–5.9 GHz notch by embedding an elliptic slot into a convex-shaped patch.

In order to avoid the interference from services working at different frequency bands, dual band-notched UWB antennas were presented [11]-[15]. In [11], by cutting an elliptical slot on the modified circular patch and an inverted G-shaped slot on the ground plane, a 3.5/5.5 GHz dual band-notched UWB antenna was presented. In [12], by cutting two L-shaped slits and an E-shaped slot with variable dimensions on the radiating patch, dual band-notch characteristics are generated. In [13], the proposed antenna generated dual band-notched function by using four rectangular-shaped slots. In [14], the proposed antenna can obtain a UWB property with dual notched band by using two U-shaped slots on the radiating patch. In these designs, the desired notched band frequencies are achieved by usually adjusting the total lengths of the etching slots, which makes the switch of the center frequency limited. Hence, in order to improve the performance of the UWB system, antennas with reconfigurable structures which exhibit switchable band notch performances are desirable. In [15], by etching two symmetrical notches on the feed-line and cutting two slots on the radiating patch and embedding two positive-intrinsic-negative (PIN) diodes along these slots, a reconfigurable ultra-wideband slot antenna with switchable single/dual band notch functions was proposed. In this structure, the change of the bias states of the PIN diodes makes the antenna capable of

Submitted On: October 30, 2016
Accepted On: December 21, 2018

exhibiting four different performances of UWB spectrum coverage. However, most reported UWB antennas were designed with no more than two notched bands, which reveals that potential interference from other narrow bands may still exist with such antennas. In [16], a wideband circular slot antenna with tri-band rejection characteristics at 2.45, 5.45, and 8 GHz was proposed by using a split ring and an inverted L-shaped slot on the circular patch. In [17], the triple band-notched characteristics, rejecting the 3.4–3.6 GHz, 5.5–6.05 GHz and 7.8–8.3 GHz frequency bands, are obtained by etching a complementary split-ring resonator (CSRR) inside the radiate patch of printed elliptical monopole antenna (PEMA) and inserting a U-Shaped slot in the ground plane respectively. Although three notched bands are obtained, it is difficult to control the bandwidth of the desired notched-bands because of strong couplings between the band-notched characteristic designs. For instance, the notched band for WiMAX (3.3-3.7 GHz) is missing and the notched band for WLAN (5.15–5.825 GHz) is not complete in [16]. The notched bands for both WiMAX (3.3-3.7 GHz) and WLAN (5.15–5.825 GHz) are not complete in [17].

In this paper, a reconfigurable UWB antenna with switchable single/dual/triple band notch functions is proposed by etching slots on the radiating patch, the ground plane, and the feedline. The proposed antenna can operate within an ultrawide band from 3.53 GHz to above 9.56 GHz. Meanwhile, the antenna can reject the frequency bands of 3.30~4.68 GHz, 5.15~6.48 GHz, and 7.25~8.54 GHz and hence avoid the interference from WiMAX, WLAN, and X-band satellite systems. Furthermore, it is observed that the notch frequencies of the antenna could be varied independently by switching PIN diode switches. The switches being either shorted or open will allow the antenna to operate at eight modes and can realize an interconversion between one UWB mode, three single band-notched modes, three dual band-notched modes, and one triple band-notched mode. Details of antenna design, the simulated and measured results are presented and discussed in the following sections.

II. ANTENNA DESIGN

The schematic configuration of the proposed microstrip-fed planar monopole antenna for triple band-notched operation is shown in Fig. 1. The slot antenna is printed on an FR-4 substrate with a relative permittivity of 4.4 and a thickness of 1.6mm and loss tangent 0.02. The antenna consists of a planar circular disc monopole with an arc H-shaped slot and is fed by a 50 ohm microstrip line. Compared to the straight-shaped H-shaped slot [18], the arc H-shaped slot can provide more degrees of freedom (such as α, R_1, L_1) for tuning the center frequency of the desired rejectband. An inverted L-shaped slot is etched on the microstrip feedline. The ground plane is reshaped as a T-shaped defected ground structure with two narrow L-shaped slots. The top corners and rectangular panes are removed to improve the impedance bandwidth and reduce the return loss. Note that, each end of arc H-shape slot is short circuit and then the arc H-shape slot can be equivalent to a half-wavelength resonator. The length of the arc H-shaped slot, l_1, can be calculated by:

$$l_1 = \frac{\lambda_g}{2} = \frac{c}{2f_{notch}\sqrt{\varepsilon_e}}, \tag{1}$$

$$\varepsilon_e = \frac{(\varepsilon_r+1)}{2}. \tag{2}$$

The narrow L-shaped slots and the inverted L-shaped slot short at one end, open at the other. They can be equivalent to quarter-wavelength resonator and the length of the slots l, can be approximately calculated by:

$$l = \frac{\lambda_g}{4} = \frac{c}{4f_{notch}\sqrt{\varepsilon_e}}, \tag{3}$$

where f_{notch} is the center frequency of the stopband, c is the speed of light, λ_g is the guide wavelength, ε_e is the effective permittivity, ε_r is the relative permittivity. Assume the center frequency of the WiMAX working frequency band is 3.6 GHz and the length of the arc H-shaped slot is about 25mm. Similarly, assume the center frequency of WLAN is 5.6 GHz and X-band satellite systems is 8.1 GHz, the length of narrow L slot is about 8mm and the inverted L-shaped slot is about 5mm. The length of the arc H-shaped slot, l_1, for 3.6 GHz resonant frequency can be derived by:

$$l_1 = 2(\alpha R_1 + R_1 - W_2). \tag{4}$$

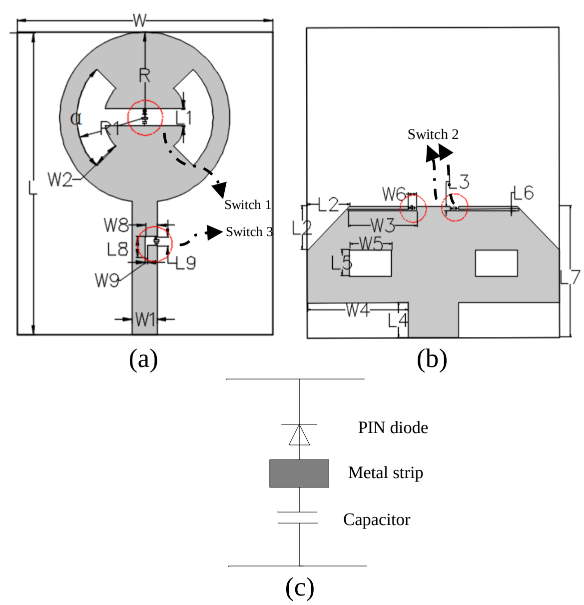

Fig. 1. Schematic configuration of the proposed UWB antenna: (a) front view, (b) back view, and (c) switch structure.

Similarly, the length of the narrow L slot, l_2, for 5.6 GHz resonant frequency and the length of the inverted L slot, l_3, for 8.1 GHz can be derived by:

$$l_2 = L_3 + W_3, \quad (5)$$

$$l_3 = L_8 + W_8. \quad (6)$$

The final triple band-notched UWB antenna design is achieved by tuning the length, width, and the slot dimensions of the radiating patch, the microstrip line, and the defected ground structure. The optimized parameter values of the proposed band-notched UWB antenna are summarized in Table 1.

Table 1: Design parameters of the proposed UWB antenna (unit: mm)

Parameter	Value	Parameter	Value
W	30	W_3	7.3
L	35.5	L_3	0.5
α	$\pi/3$	W_4	12
R	10	L_4	4
R_1	8	W_5	5
W_1	3	L_5	3
L_1	2	W_6	1
W_2	3.2	L_6	0.2
L_2	5	L_7	15
W_8	1.5	L_8	2.5
W_9	0.3	L_9	1

By etching an arc H-shaped slot on the circular radiating patch, the antenna can avoid the interference from IEEE 802.16 WiMAX system operating at 3.3–3.7 GHz. By etching two narrow L-shaped slots on the defected ground plane, a second band notch function, which can prevent the influence from IEEE 802.11a WLAN system operating at 5.15–5.825 GHz, can be achieved. Further, in order to avoid the interference from X-band satellite signals operating at 7.25-7.75 GHz and 7.9-8.4 GHz, a third stopband is implemented by etching an inverted L-shaped slot on the microstrip feedline.

Furthermore, the proposed antenna can realize the switchable band notch characteristics by introducing PIN diode switches. Since each slot acts as a resonator and the resonant frequency mainly depends on its length, PIN diode switches are used in the slots to change their effective electrical length. In order to apply DC voltage to PIN diodes, metal strips are used inside the slots. Moreover, a 100-pF blocking capacitor is placed in each slot to create RF connection of PIN diode and isolate the RF signal from DC. Therefore, the band-notched function can be flexibly controlled by the status of the switches, which will be discussed in detail in the next section.

III. BAND-NOTCHED FUNCTION ANALYSIS

A. Triple band-notched function

Figure 2 illustrates the return loss of the proposed antenna structure. It is clearly evident from this figure (curve (i)) that by cutting an arc H-shaped slot on the radiating patch, one stopband at the low frequency is excited. Curve (ii) illustrates that two stopbands (one at the same low frequency and the other at the medium frequency) are excited by cutting the arc H-shaped slot on the radiating patch and two narrow L-shaped slots on the ground plane. Furthermore, curve (iii) illustrates that a third stopband at the high frequency is excited by etching an inverted L-shaped slot on the microstrip feedline. Therefore, by cutting an arc H-shaped slot on the radiating patch, narrow L-shaped slots on the ground plane, and an inverted L-shaped slot on the microstrip feedline, three stopband rejections will be formed with a center frequency of each stopband at 3.6 GHz, 5.6 GHz, and 8.1 GHz, respectively.

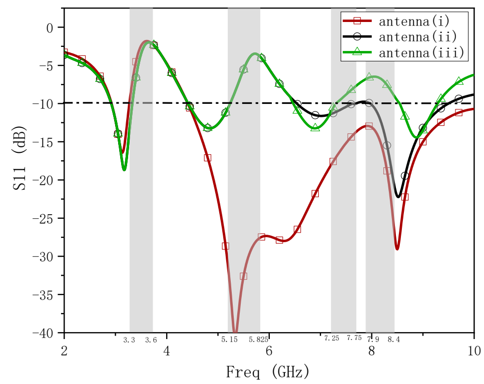

Fig. 2. Simulated return loss against frequency for the various configurations. (i) single band-notched antenna by cutting an arc H-shaped slot on the radiating patch; (ii) dual band-notched antenna by cutting an arc H-shaped slot on the radiating patch and two narrow L-shaped slots on the ground plane; (iii) triple band-notched antenna by cutting an arc H-shaped slot on the radiating patch, two narrow L-shaped slots on the ground plane, and an inverted L-shaped slot on the microstrip feedline.

To clarify the phenomenon behind the excitation of stopbands, Fig. 3 presents the input impedance of the proposed antenna with triple band-notched functions. In this figure, the input resistance and the input reactance keep the normal value except for the notch bands. When the working frequency is set at 3.6 GHz, 5.6 GHz and 8.1 GHz which are the center frequencies of the stopband, the proposed antenna would be at a state of parallel resonance. The input resistance is maximum and the input reactance vanishes when the antenna works at the state of parallel resonance. The equivalent circuit of the proposed antenna with triple band-notched function is presented in Fig. 4. As shown in Fig. 4, the proposed antenna could be equivalent to a combination of three parallel resonant circuits. When the working frequency is set at 3.6 GHz, the first parallel resonant circuit sets up a resonance. Thus, a total impedance mismatch occurs between the feed line and radiating patch, and the first band-notched characteristic is generated. Similarly, the second parallel resonant circuit resonates at 5.6 GHz and the third at 8.1 GHz.

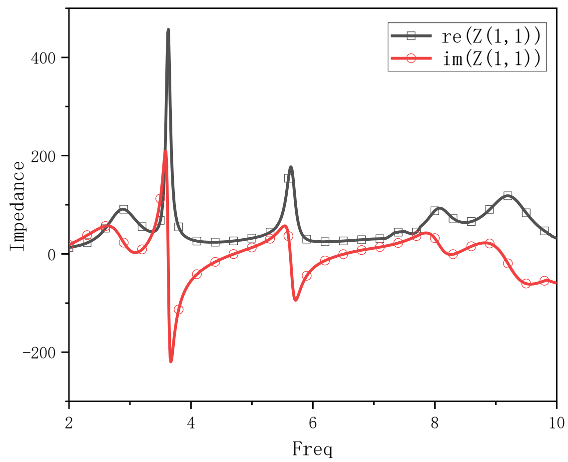

Fig. 3. Impedance of the proposed antenna with triple band-notched function.

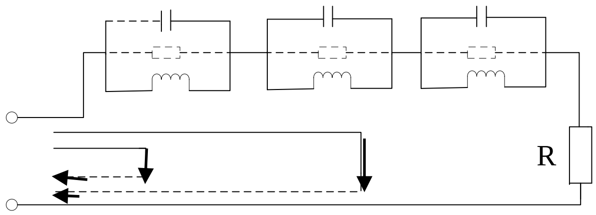

Fig. 4. Equivalent circuit of the proposed antenna with triple band-notched function.

In order to further explain the triple band-notched function resulting from slotted structure, the simulated surface current distribution for the proposed antenna at the resonant frequencies of 3.6, 5.6, and 8.1 GHz are shown in Fig. 4. It can be observed from the figure that the current distributions are different at the three notched bands. In particular, when the antenna operates at 3.6 GHz, as shown in Fig. 5 (a), most of the currents are concentrated near the arc H-shaped slot on the radiating patch; As shown in Fig. 5 (b), the currents are mainly distributed around two L-shaped slots on the ground plane when the antenna works at 5.6 GHz; when the antenna works at 8.1 GHz, as shown in Fig. 5 (c), the currents are mainly concentrated around the inverted L-shaped slot. Therefore, the antenna resonates at these frequencies due to the band-notched functions of these slotted structures.

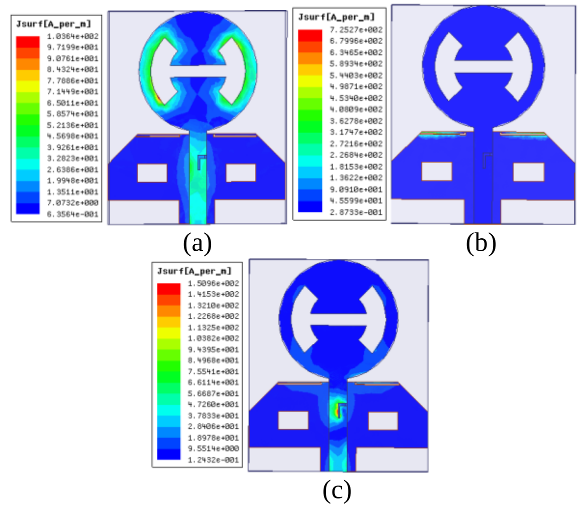

Fig. 5. Simulated surface current distributions on the radiation patch for the proposed antenna at: (a) 3.6 GHz, (b) 5.6 GHz, and (c) 8.1 GHz.

B. Switchable single/dual/triple band-notched function

As shown in Fig. 1, the controllability of band-notched functions is realized by adding one PIN diode in each slot. Since each slot act as a resonator and the resonant frequency mainly depends on its length, PIN diode switches are used in the slots to change their effective electrical length. Thus, each stopband being existing or not can be controlled by biasing PIN diode in the slot, respectively.

The PIN diode in the arc H-shaped slot which excites one stopband at the low frequency is called switch 1 and the switch 1 being shorted or open controls whether the stopband at the low frequency exists or not. Since two narrow L-shaped slots work together to excite one stopband at the medium frequency, the two PIN diodes in the two slots are called switch 2 and the switch 2 being shorted or open controls whether the stopband at the medium frequency exists or not. The PIN diode in the inverted L-shaped slot on the feedline which excites one stopband at the high frequency is called switch 3 and the switch 3 being shorted or open controls whether the stopband at the high frequency exists or not. When all three switches are open, the slots can excite three stopbands normally and the proposed antenna works at the triple-band-notched mode. When none of three switches is open, the three slots in the antenna cannot work properly and the proposed antenna works at the UWB mode. When one of three switches is open, the antenna works at single band-notched mode. The antenna works at the dual-band-notched mode when two of three switches are open. For the proposed antenna, eight operating modes are investigated, and their corresponding diode states are shown in Table 2.

Table 2: The switch states and stopbands when the proposed antenna work at different modes

Mode	Switch 1	Switch 2	Switch 3	Stopbands
1	0	0	0	none
2	1	0	0	3.28~4.41 GHz
3	0	1	0	5.46~6.55 GHz
4	0	0	1	7.76~8.25 GHz
5	1	1	0	3.30~4.42 GHz, 5.15~6.54 GHz
6	1	0	1	3.30~4.65 GHz 7.7~8.34 GHz
7	0	1	1	5.4~6.61 GHz, 7.25~8.46 GHz
8	1	1	1	3.30~4.68 GHz, 5.15~6.48 GHz, 7.25~8.54 GHz

1: Open, 0: Shorted.

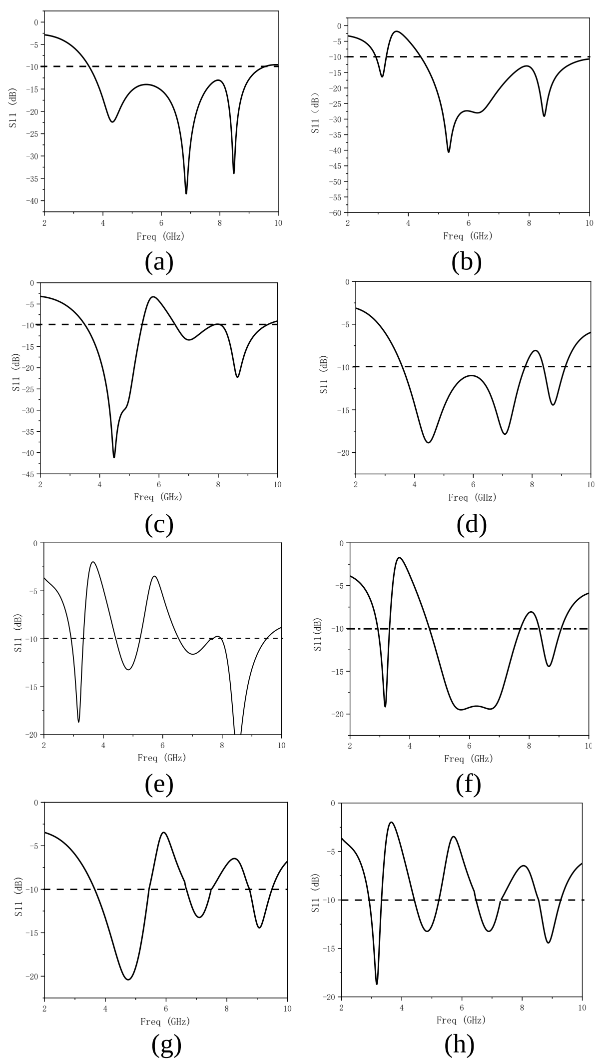

Fig. 6. Simulated return loss of the proposed antenna: (a) Mode 1, (b) Mode 2, (c) Mode 3, (d) Mode 4, (e) Mode 5, (f) Mode 6, (g) Mode 7, and (h) Mode 8.

Figure 6 presents the return loss of the antenna in each mode.

IV. EXPERIMENTAL RESULTS AND DISCUSSIONS

To verify the proposed design, the antenna is practically fabricated on FR-4 substrate with the dimensions of 35.5mm×30mm×1.6mm, and the photograph of the fabricated antenna is shown in Fig. 7. The measured results are obtained by using an Agilent N5230A vector network analyzer and an anechoic chamber. For brevity, Fig. 8 only presents the measured return loss curves of three typical modes among the eight modes, showing a good agreement with the simulated return loss in Fig. 2. The slight deviation may be due to fabrication errors, feed wires, and imperfections of components. It is found that proposed design can reject the frequency band of 3.08~4.22 GHz and avoid the interference from WiMAX when the switch 1 is open, switch 2 and switch 3 are shorted. The proposed antenna can reject frequency bands of 3.1~4.23 GHz and 5.17~6.12 GHz and avoid the interferences from WiMAX and WLAN when switch 1 and switch 2 are open, switch 3 is shorted.

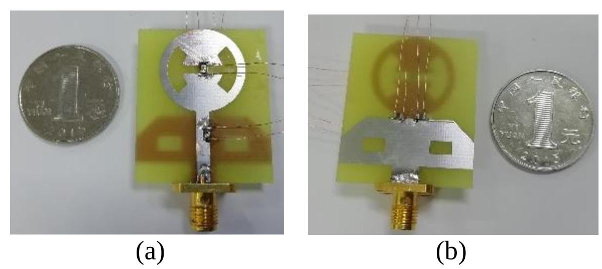

Fig. 7. Photo of fabricated switchable band-notched UWB antenna: (a) front view and (b) back view.

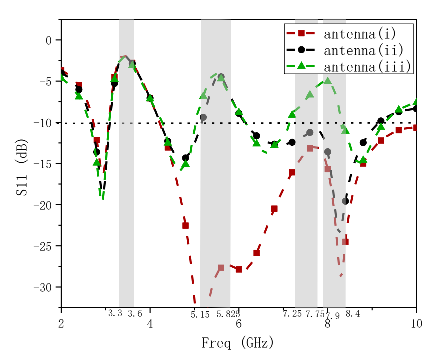

Fig. 8. Measured return loss against frequency for the various configurations. (i) single band-notched antenna by opening switch 1, shorting switch 2 and switch 3; (ii) dual band-notched antenna by opening switch 1 and switch 2, shorting switch 3; (iii) triple band-notched antenna by opening switch 1, switch 2, and switch 3.

The proposed antenna can reject frequency bands of 3.08~4.29 GHz, 5.03~6.15 GHz and 7.15~8.3 GHz and avoid the interferences from WiMAX, WLAN, and X-band satellite systems when switch 1, switch 2, and switch 3 are open.

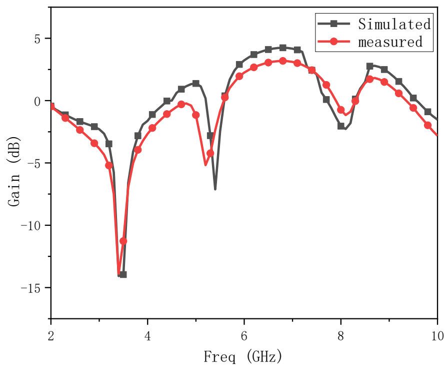

Fig. 9. Gain of the proposed antenna with triple band-notched function.

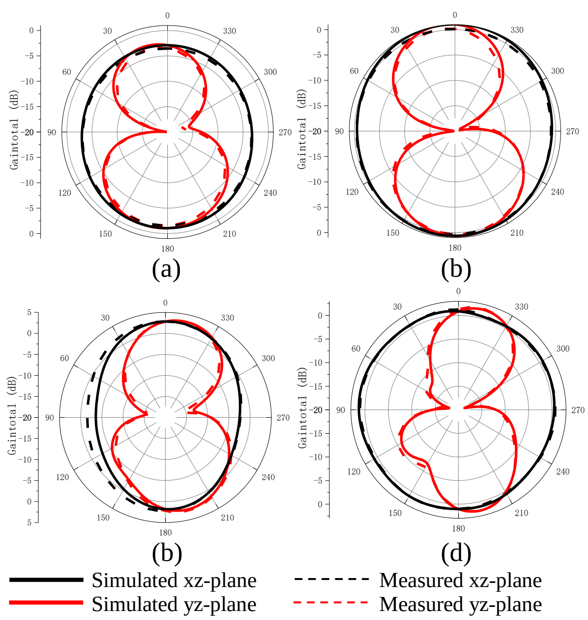

Fig. 10. Simulated and measured radiation patterns at: (a) 2.8 GHz, (b) 4.9 GHz, (c) 6.8 GHz, and (d) 8.7 GHz frequencies for the proposed antenna with triple band-notched function.

Figure 9 shows the measured and simulated gain variations with the frequency for the proposed triple band-notched antenna. Three sharp decreases of gain values are observed in the notched bands at 3.5, 5.5, and 8 GHz, respectively. Figures 10 (a-d) show the 2-D far-field radiation patterns in the E- plane (yz-plane) and H-plane (xz-plane) at sampling frequencies of 2.8 GHz, 4.9 GHz, 6.8 GHz, and 8.7 GHz respectively. In these figures, good omnidirectional radiation characteristics are observed. The results show that the proposed antenna performs well in four different passbands and meets the requirements of UWB communications.

V. CONCLUSION

A reconfigurable ultrawide band (UWB) antenna with switchable single, dual, and triple band notch functions is presented in this paper. The low frequency band-notched function is formed by an arc H-shaped slot on the radiating patch; the medium frequency band-notched function is formed by two narrow L-shaped slots on the ground plane; and the high frequency band-notched function is formed by an inverted L-shaped slots on the microstrip feedline. The proposed antenna can avoid the interference from WiMAX, WLAN, and X-band satellite systems. Further, by introducing switch modes on the slots, the antenna offers eight working modes and can realize an interconversion between one UWB mode, three single band-notched modes, three dual band-notched modes, and one triple band-notched mode. The results of the return loss and the input impedance show that the designed bandwidth with good band rejection is presented. Nearly omnidirectional radiation patterns and desirable gain are also presented to verify the satisfactory performance of the proposed antenna.

ACKNOWLEDGMENT

This work was supported in part by the National Natural Science Foundation of China under Grant No. 61801521, in part by the Natural Science Foundation of Hunan Province under Grant No. 2018JJ2533, and in part by the Fundamental Research Funds for the Central Universities under Grant No. 2018gczd014.

REFERENCES

[1] Federal Communications Commission. First report and order in the matter of revision of part 1-5 of the commission rules regarding ultra-wideband transmission systems. USA: FCC, 2002.

[2] A. Kerkhoff and H. Ling, "Design of a planar monopole antenna for use with ultra-wideband (UWB) having a band-notched characteristic," *Proc. IEEE AP/S Int. Symp. Dig.*, Columbus, OH, vol. 1, pp. 830-833, June 2003.

[3] H. Schantz, G. Wolenec, and E. Myszka, "Frequency notched UWB antenna," *Proc. IEEE Conf. Ultra Wideband Syst. Technol.*, pp. 214-218, Nov. 2003.

[4] D.-Z. Kim, W.-I. Son, W.-G. Lim, H.-L. Lee, and J.-W. Yu, "Integrated planar monopole antenna with microstrip resonators having band-notched characteristics," *IEEE Transactions on Antennas and Propagation*, vol. 58, pp. 2837-2842, 2010.

[5] S. Ghosh, "Band-notched modified circular ring

monopole antenna for ultrawideband applications," *IEEE Antennas and Wireless Propagation Letters*, vol. 9, pp. 276-279, 2010.

[6] S.-J. Wu, C.-H. Kang, K.-H. Chen, and J.-H. Tang, "Study of an ultrawideband monopole antenna with a band-notched open-looped resonator," *IEEE Transactions on Antennas and Propagation*, vol. 58, pp. 1890-1897, 2010.

[7] A. Ghobadi, C. Ghobadi, and J. Nourinia, "A novel band-notched planar monopole antenna for ultra-wideband applications," *IEEE Antennas and Wireless Propagation Letters*, vol. 9, pp. 608-611, 2009.

[8] J. B. Jiang, Y. Song, Z. H. Yan, X. Zhang, and W.Wu, "Band-notched UWB printed antenna with an inverted-L-slotted ground," *Microw. Opt. Technol. Lett.*, vol. 51, no. 1, pp. 260-263, Jan. 2009.

[9] K. Ruchandani and M. Kumar, "A novel CPW fed octagonal aperture antenna with back patch for UWB applications," *International Conference on Nascent Technologies in the Engineering Field (ICNTE) - Navi Mumbai*, India, 2015.

[10] Z.-J. Tang, X.-F. Wu, and J. Zhan, "Novel compact band-notched UWB antenna using convex-shaped slot patch," *Microw. Opt. Technol. Lett.*, vol. 57, no. 1, pp. 201-203, Jan. 2015.

[11] G. Srivastava and A. Mohan, "A planar UWB monopole antenna with dual band notched function," *Microw. Opt. Technol. Lett.*, vol. 57, no. 1, pp. 99-104, Jan. 2015.

[12] M. Mehranpour, J. Nourinia, C. Ghobadi, and M. Ojaroudi, "Dual band-notched square monopole antenna for ultrawideband applications," *IEEE Antennas and Wireless Propagation Letters*, vol. 11, pp. 172-175, 2012.

[13] Z. Esmati and M. Moosazadeh, "Dual band-notched small monopole antenna with bandwidth enhancement by means of defected ground structure (DGS) for UWB application," *Applied Computational Electromagnetics Society Journal (ACES)*, vol. 30, no. 6, pp. 619-625, 2015.

[14] A. Sharma and M. M. Sharma, "An UWB antenna design with dual band notched characteristic using U-shaped slots," *International Conference on Signal Processing & Communication*, *IEEE*, 2017.

[15] B. Badamchi, J. Nourinia, C. Ghobadi, and A. Shahmirzadi, "Design of compact reconfigurable ultra-wideband slot antenna with switchable single/dual band notch functions," *IET Microwaves, Antennas & Propagation*, vol. 8, no. 8, pp. 541-548, 2014.

[16] J. Yeo, "Wideband circular slot antenna with tri-band rejection characteristics at 2.45/5.45/8 GHz," *Microwave and Optical Tech. Lett.*, vol. 50, pp. 1910-1914, 2008.

[17] J.-Y. Deng, Y.-Z. Yin, S.-G. Zhou, and Q.-Z. Liu, "A novel triple band-notched monopole antenna," *Journal of Electromagnetic Waves and Application*, vol. 23, pp. 139-147, 2009.

[18] X. L. Bao and M. J. Ammann, "Printed UWB antenna with coupled slotted element for notch-frequency function," *International Journal of Antennas and Propagation*, 2008.

Jian Dong received the B.S. degree in Electrical Engineering from Hunan University, Changsha, China, in 2004, and the Ph.D. degree in Electrical Engineering from Huazhong University of Science and Technology, Wuhan, China, in 2010. He is now an Associated Professor and the Vice Director of Communications and Networks Research Center at the Central South University (CSU), Changsha, China. He has been a Visiting Scholar at the ELEDIA Research Center of the University of Trento, Italy, from March 2016 to March 2017. His research work is mainly focused on antenna array synthesis, ultrawide band/multi-band antennas, and numerical optimization techniques. He holds about 30 innovation patents and has published six books and over 100 peer reviewed papers on international journals and conferences.

Shan Wang received the B.S. degree in Communication Engineering from Center South University, Changsha, China, in 2018. She is now pursuing her M.S. degree at Center South University, Changsha, China. Her current research interests focus on reconfigurable antennas, ultrawide band/multi-band antennas. She has published two journal/conference papers.

Guoqiang Hu received the B.S. degree in Electrical Engineering from Anhui Normal University, Wuhu, China, in 2014, and the M.S. degree in Electrical Engineering from Center South University, Changsha, China, in 2017. He is now a Senior Antenna Engineer at Transsion Holdings Limited Inc., Shanghai, China. His current research interests focus on wideband/multiband antenna designs. He has published three journal papers and holds two innovation patents.